Journal of Inorganic and Organometallic Polymers and Materials (2022) 32:4589–4600
https://doi.org/10.1007/s10904-022-02465-z

RESEARCH

Radiation Synthesis of Green Nanoarchitectonics of Guar Gum-Pectin/Polyacrylamide/Zinc Oxide Superabsorbent Hydrogel for Sustainable Agriculture

Asmaa Sayed[1] · Mai M. Mohamed[1] · Manar El-Sayed Abdel-raouf[1,2] · Ghada A. Mahmoud[1]

Received: 25 July 2022 / Accepted: 5 August 2022 / Published online: 16 August 2022

Abstract
In the current study, the performance of superabsorbent hydrogel composites comprised of Guar gum-Pectin/Polyacrylamide/ZnO crosslinked with gamma irradiation (10 kGy) has been investigated for sustainable agriculture. The claimed composites (GG/PC/PAAm/ZnO_x) were characterized by FTIR, TGA, and AFM. The swelling capacity data reveal that the equilibrium water swelling (EW) of the composites was increased by increasing the ZnO content from 600 to 1050 g/g for zero to the highest concentration of ZnO, respectively. Furthermore, the physical properties of the soil mixed with the hydrogels were improved; water holding capacity (WHC) increased to 66% and water retention (WR) kept at 15% after 20 days. The composites showed a good degradability in the biodegradation test. They also portrayed super-absorption capacity at three swelling/deswelling cycles. This advancement is important for reducing water consumption through the irrigation of arid lands. The prepared composites were proved as excellent candidates in sustainable agriculture applications.

Keywords Guar gum · Pectin · Sustainable agriculture · Swelling · Water holding capacity · Zinc oxide

1 Introduction

One of the most important bases of bioeconomy is replacing fossil-based materials with environmentally friendly sustainable resources [1, 2]. In this regard, efforts are directed to employ different biopolymers in industrial, agricultural and biomedical applications [3]. Moreover, different biomass finds great importance in many novel applications such as electrode material for super capacitors [4], capacitive deionization perfromance [5], electromangetic wave absorber [6] and as electrocatalyst [7].

Plant-derived polymer such as cellulose, starch, pectin and guar gum are more advantageous than those of animal origin due to their abundancy, higher functionalities and ease of extraction and handling [8].

On the other hand, the continuous depletion of freshwater resources accompanied by an incessant increase in world's population is a serious global problem especially due to climate change. Water is the principal demand for agriculture, cultivation and crop production [9, 10]. One of the most effective solutions to reduce water consumption is using materials with high water absorption and good retention capacities called superabsorbent hydrogels [2]. Superabsorbent hydrogels consist of three-dimensional (3D) hydrophilic polymer networks that have the potential to absorb and hold a large amount of water and aqueous solution [11, 12]. They are being used for water management aimed at agricultural development [13], as they can absorb and store water many times more from its particular volume and perform the function of reservoirs with water and increase water retention. This feature helps reduce water stress in plants and ensure high plant productivity, which leads to increased growth and yield [14]. The use of polymeric hydrogel can improve water and fertilizer efficiency. Also, superabsorbent polymers improve some physical properties of the soil. Synthetic hydrogels based on acrylates and acrylamides show high mechanical strength and the potential to absorb significant quantities of water. Due to the problem of their biodegradability, they are being blended with biopolymers such as alginate, agar, cellulose, chitosan, gum and starch

✉ Manar El-Sayed Abdel-raouf
drmanar770@yahoo.com

[1] Polymer Chemistry Department, National Center for Radiation Research and Technology, Egyptian Atomic Energy Authority, Cairo, Egypt

[2] Egyptian Petroleum Research Institute, 1Ahmed Elzomor street, Nasr city, Cairo 11727, Egypt

[15]. Blending of natural polymer with a synthetic one has received increasing attention in last decades as it can reduce pollution of the synthetic polymers and also has a wide range of potential applications in different fields [16].

Natural polymers, especially the polysaccharides, have been widely used particularly in environmental applications due to their attractive issues such as low-cost, abundance, renewability, and biodegradability [17]. Guar gum (GG) is a galactomannan polysaccharide with comprised of main chain of mannose units joined by β-D (1→4) linkages having β-D galactopyranose units attached to this linear chain by (1→6) linkages. The guar molecule possesses numerous hydroxyl groups that can form extensive intra and inter hydrogen bonding which make guar material one of the best- known natural polymer as gel forming material with excellent gelation property [18]. Pectin (PC) is another highly functional natural polymer [19]. At present, pectin is believed to consist mainly of linear D-galacturonic acid units, joined by a-(1–4) glycosidic linkage. These uronic acids have carboxyl groups, some of which are naturally present as methyl esters [20]. Combining these two natural polymers in a three-network structure fulfills maximum benefits from the advantages of both polymers. Moreover, incorporating an inorganic core such as zinc oxide reserves the cohesion of the gel matrix and keeping the gel consistency while absorbing huge amount of water. Therefore, the main target is to constitute a series green superabsorbent hydrogel for water retention and soil amendment. This was achieved by a green synthetic methodology based on irradiation polymerization and crosslinking of guar gum/Pectin grafted with polyacrylamide with a core of zinc oxide. The gamma route fulfills several advantages such as clean simple technique, high-productivity, low energy, and low-cost process that leads to less contamination and fewer byproducts [21, 22]. Radiation treatment can also introduce better surface crosslinking between natural and synthetic polymers by enhancing the formation of free macroradicals which finally lead to formation of crosslinked structure [23]**.** Moreover, the hydrogel composites were characterized via different techniques including infrared spectroscopy, Atomic force microscopy, and thermal analysis. The swelling properties of the prepared hydrogel composite GG-PC/Pam/ZnO_x were verified in different saline solutions. Water retention and degradation rate of prepared superabsorbent composites were also evaluated. The swelling performance of the optimum hydrogel was investigated at three swelling/deswelling cycles.

2 Experimental Section

2.1 Materials

Pectin powder from apple [Poly-D-galctouronic acid methyl ester (PC)] with degree of esterification (DE) of 50–75% was purchased from Sigma-Aldirch (China), The viscosity average molecular weight (Mv) of this pectin grade was informed to be 1.538×10^5 g/mol [24].Ultra-pure Guar gum powder (GG) with viscometric molecular weight 2.5×10^5 g/mol was provided from Sigma-Aldrich and used without further purification. Acrylamide (AAm) of purity 99.9%, and zinc oxide nanopowder < 50 nm particle size molecular weight 81.39 surface area 10–25 m^2/g were supplied from Sigma Aldirch, UK. Double-distilled water was used for the preparation of all solutions in this study. All other reagents were in analytical grade and used without any further purification.

2.2 Sandy Soil

The sandy soil sample was collected from different points at Suez Road to the direction of Sokhna, Cairo, Egypt. Physical and chemical properties of the studied soil samples, were determined as described by Hasija et al. [25] (The data are presented in Table 1).

2.3 Preparation of GG-PC/PAAm Hydrogel

A simple protocol was applied. Briefly, 1.3 g Guar gum and 0.7 g of pectin were separately dissolved in 46.2- and 46.8-ml deionized water, respectively and stirred at 50 °C till complete solubility. Then, the two solutions were added together. Afterwards, 5 g of Acrylamide monomer was added to the GG-PC solution then the solution was stirred at ambient temperature until complete homogeneity, where the total polymer and monomer content was 7 wt%. Then 20 mL of the resulted solution was poured into glass test tubes each and they were exposed to ^{60}Co-gamma irradiation of irradiation doses 10 kGy; (this irradiation dose was sufficient to form a gel% ≈ 99.9%), the resultant hydrogels were coded as *GG-PC/PAAm/ZnO_0*. The prepared hydrogel was sliced into almost identical discs and incubated overnight in distilled water at 80 °C, to remove the unreacted monomer then dried at room temperature.

2.4 Preparation of GG-PC/PAAm/ZnO_x Composites

The hydrogel composites were prepared via a facile methodology. ZnO solution (0.1 gm in 50 mL of deionized water) was sonicated at 25 °C for 30 min then, different volumes of ZnO solution (0,1, 3, 5 &7 mL) were added to 20 mL of GG-PC/AAm solution with continuous stirring for 10 min to assure complete homogeneity. The resulted solutions were then transferred into glass test tubes and subjected to ^{60}Co-gamma rays at 10 kGy irradiation dose for synthesis of the GG-PC/PAAm/ZnO_0, GG-PC/PAAm/ZnO_1, GG-PC/PAAm/ZnO_3, GG-PC/PAAm/ZnO_5, and GG-PC/PAAm/ZnO_7 respectively.

Table 1 Some chemical and physical characteristics and available nutrients for the investigated soil

Soil physicochemical properties								
Particle size distribution (%)			Textural grade	pH	OM (%)	$CaCO_3$ (%)		CEC (cmol/Kg)
Sand	Silt	Clay						
83.5	11.3	5.2	Sandy	8.21	0.71	12.11		9.15
Soil salinity								
EC (dSm^{-1})	Soluble cations (meq/L)				Soluble anions (meq/L)			
	Na^+	K^+	Ca^{++}	Mg^{++}	Cl^-	$(HCO_3)^-$	$(CO_3)^{-2}$	$(SO_4)^{-2}$
1.56	7.11	0.33	4.02	1.72	8.12	2.99	0.78	4.34
Soil available nutrients (mg/kg)								
Macronutrients					Micronutrients			
N	P	K	S		Fe	Cu	Zn	Mn
55.12	3.17	811.17	6.78		3.12	0.52	0.96	5.79

2.5 Characterization

Fourier transform-infrared spectroscopy (Bruker, Unicom infra-red spectrophotometer, Germany) was used to identify the functional groups at 400–4000 cm^{-1} wavelength range. The KBr was ground and mixed with the dried sample, and the mixture was pressed into thin plates for infrared testing. The surface morphology and topography of the composites were monitored by AFM, Flexaxiom Nanosurf, C3000 at the dynamic mode (non-contact) to confirm chemical modification and to detect the changes accompanying the swelling process. The AFM examinations were conducted at room temperature using a NCLR silicon cantilever with rectangular shape and a resonance frequency of 9 kHz. The thermal behavior of the prepared composites was verified via a thermogravimetric analyzer (Perkin-Elmer Co., USA) at a heating rate of 15 °C $min^{-1}$from 30 to 600 °C under a nitrogen atmosphere.

2.6 Swelling Behavior in Different Media and Equilibrium Water Absorbance of GG-PC/PAAm/ZnO_x Superabsorbent Composites

The equilibrium water absorbance and swelling of synthesized hydrogel composites were measured by immersing a circular disc of dried hydrogel in 250 ml of distilled water to attain maximum swelling equilibrium state (Q_{eq}) [26]. The swollen gel was taken off the water and gently dried with a tissue paper to remove the excess water, then it was weighed. The Equilibrium water absorbance was calculated according to the Eq. (1):

$$Q_{eq}(\%) = \frac{w_s - w_d}{w_d} \times 100 \quad (1)$$

where Q_{eq} is the equilibrium water absorbance (g/g) (EW) at time t (min), W_s is swollen hydrogel (g), and W_d is dried hydrogel (g). The swollen gels were filtered, and the Equilibrium water absorbance was calculated according to the above Eq. (1). Moreover, swelling behavior of the GG-PC/PAAm/ZnO_x hydrogel composites was verified versus different variables: Different saline concentration (1.7, 3.4, 5.1, 6.8, 8.6 mmol/L), various pH solutions ranged from 1.0 to 11.0, temperature range 25-45 °C.

2.7 Water Retention (WR) and Water Holding Capacity (WHC) of Soil with GG-PC/PAAm/ZnO_x Composite

The ability of the prepared composites to modify the soil holding and retaining capacity was monitored by calculating the WHC% and WR% of soil mixed with different concentrations of GG-PC/PAAm/ZnO_x. They were measured by taking 100 g of dry soil (A) as blank, and 100 g of dry soil mixed with (1, 2 and 3%) g of GG-PC/PAAm/ZnO_0 and GG-PC/PAAm/ZnO_7 as (B) and (C) respectively. Each sample was placed in a sealed tube with 200-mesh nylon fabric and weighed (W_O). The three soil samples (A), (B), and (C) samples were soaked with distilled water until saturation, and then the samples were weighed again ($\mathbf{W_1}$). The WHC % of the soil was calculated using Eq. (2).

$$WHC\% = \frac{w_1 - w_o}{w_o} \times 100 \quad (2)$$

The WR % of the soil with the GG-PC/PAAm/ZnO_x composite was calculated by Eq. (4), and the soil samples were kept under the same conditions and weighed every 2 days ($\mathbf{W_i}$) for 20 days.

$$\mathrm{WR}\% = \frac{W_i - W_o}{W_1 - W_o} \times 100 \tag{3}$$

2.8 Biodegradation Rate (BR) of GG-PC/PAAm/ZnO_x Composite in Soil

The degradation rate of the GG-PC/PAAm/ZnO_0 GG-PC/PAAm/ZnO_7 composites was determined by measuring the weight loss of the composites with the incubation time in soil. The GG-PC/PAAm/ZnO_x composite (0.1 g) was placed in perforated plastic bags and then buried about 5 cm under the surface of the soil and incubated for up to 30 days. The bags were then picked out each 2 days washed and dried until constant weight, and then the GG-PC-PAAm/ZnO_x composite was weighed to calculate the weight loss with Eq. (4).

$$\mathrm{BR}\% = \frac{W_1 - W_o}{W_o} \times 100 \tag{4}$$

where: W_o and W_i are the weights of the hydrogel composites before and after degradation (g), respectively.

2.9 Swelling/Deswelling Study

The reusability study was conducted at three swelling/deswelling cycles. A fixed weight of the composite (0.1 gm) was placed in an excessive amount of fresh water and allowed to reach maximum swelling at ambient temperature. Then, it is picked up and weighed. Afterwards, the swelled hydrogel is placed in an oven at 100 °C until reaching its original weight. This test is repeated for three times. The maximum water absorbance is calculated according to Eq. 5.

$$Q_{\max}(\%) = \frac{W_s - W_d}{W_d} \times 100 \tag{5}$$

where Q_{max} is the maximum water absorbance (g/g) (EW) at time t (min), W_s is swollen hydrogel (g), and W_d is dried hydrogel (g).

3 Results and Discussion

3.1 Synthesis of Green Composites

A green gamma irradiation is applied to generate macroradicals on the reactive groups of guar gum and pectin. These macroradicals are crosslinked with interchain of acrylamide to form the three- dimensional structure that can hold and retain water molecules. Zinc oxide particles are incorporated to keep the consistency of the hydrogel during swelling/deswelling process. The proposed reaction is given in Scheme 1. The initial step is the formation of guar gum and pectin macroradicals initiated by the gamma irradiation. The acrylamide radicals are also formed by the same mechanism. The radical formation step is followed by crosslinking and network formation. Finally, zinc oxide is chelated with the amine groups of polyacrylamide. This mechanism is proposed by other investigators for irradiation crosslinking of different carbohydrate polymers [27, 28]. The photochemical initiation and crosslinking is highly favoured over thermochemical process, particualry at adjusted dose and controlled conditions.

3.2 Fourier Transform Infrared spectroscopy (FT-IR)

FT-IR spectra of GG, PC, GG-PC/PAAm/ZnO_0 and GG-PC/PAAm/ZnO_7 are shown in Fig. 1. The spectrum of GG showed a broad band at 3363 cm^{-1} due to the stretching vibration of—OH groups. The band at 1637 cm^{-1} is due to ring stretching of mannose. The bands at 2897 cm^{-1}, 1395 cm^{-1}, 1117 cm^{-1} and 1004 cm^{-1} correspond to C–H stretching mode, –C–H asymmetric bending, C–O–C stretching and C–O stretching vibrations respectively. [29].

The FTIR spectrum of PC also showed the broad band of—OH groups at 3334 cm^{-1}. The asymmetrical stretching band of C–H appeared at 2931 cm^{-1}. The bands of C = O and C–O of glycosidic bond was observed at 1731 cm^{-1} and 1008 cm^{-1} [30], respectively. The FTIR spectrum of GG-PC/PAAm/ZnO_0 hydrogel showed shifting and reduction the intensity of the band of—OH group due to the formation of the crosslink structure in the hydrogel. The band of C = O group is shifted to 1603 cm^{-1} and become more intense due to the presence of amide group of PAAm. Almost the band of C–O disappeared, which also confirmed the formation of the hydrogel crosslinking structure. The FT-IR spectrum of PC-GG/PAAm /ZnO_7 showed that the C = O stretching band of pectin has shifted from 1603 cm^{-1} to 1627 cm^{-1} because of interaction with ZnO [31]. The other bands were also slightly shifted due to bonding between ZnO and polymeric matrix. This confirmed the successful formation of the nanocomposite.

3.3 Atomic Force Microscopy (AFM)

AFM is a modest tool for topography charcaterization of different material. It is used in describing the surface of hydrogels in previous works [10, 32]. In this work, the AFM is used to study the surface topography, the porous structure, and the height of GG-PC/PAAm/ZnO_0, GG-PC/PAAm/

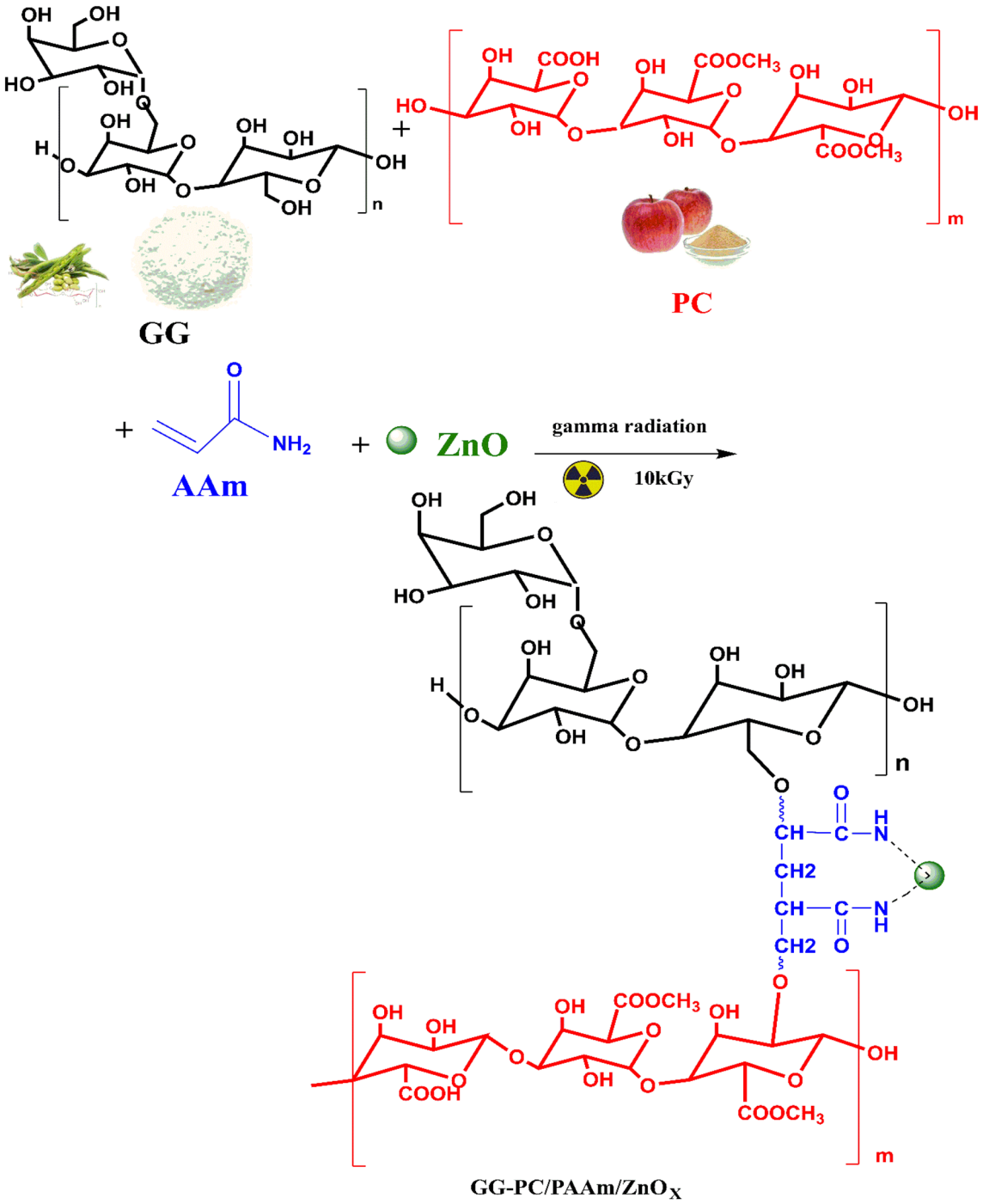

Scheme 1 Proposed reaction for hydrogel composite synthesis

ZnO_3, and GG-PC/PAAm/ZnO_7 (Fig. 2a–c) to investigate the effect of the addition of zinc oxide on the porosity and the pore volume of the prepared hydrogel composites. The images revealed that the height increases by the inclusion of zinc oxide in the composite matrix, which reflected the growth in the pore volume. The height measurements were found 0.51 nm, 0.92 nm, and 31.8 nm for GG-PC/PAAm/ZnO_0, GG-PC/PAAm/ZnO_3, and GG-PC/PAAm/ZnO_7, respectively. However, very wide pores are not suitable for retaining the water absorbed by the hydrogel. Therefore, it is expected from the AFM data that the maximum swelling will be achieved by GG-PC/Pam/ZnO_7 hydrogel composite. Moreover, the humpy surface morphology resulting from the inclusion of zinc oxide indicated the increase in the effective

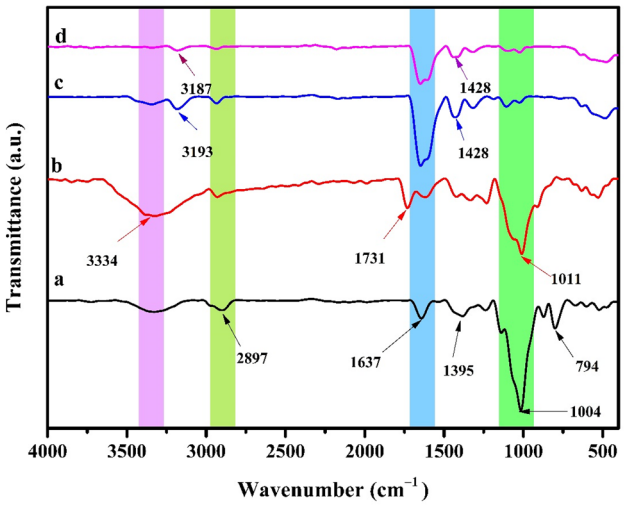

Fig. 1 FTIR spectra of: (a) GG, (b) PC, (c) GG-PC/PAAm/ZnO_0 and GG-PC/PAAm/ZnO_7

surface area, which guarantees better absorption and swelling [23].

3.4 Thermogravimetric Analysis (TGA)

The TGA thermograms of GG-PC/PAAm/ZnO_0, GG-PC/PAAm/ZnO_3 and GG-PC/PAAm/ZnO_7 are provided in Fig. 3. It is observed that the thermal degradation pattern includes three decomposition stages. The first decomposition stage was observed at 175 °C due to the elimination of the hydrated water. The second decomposition stage was observed at 295 °C due to the elimination of side groups. The third decomposition stage is due to decomposition of the backbone matrix 300–558 °C and the weight remaining (%) about 25% at 600 °C. On the other hand, the incorporation ZnO nanoparticle (GG-PC/PAAm/ZnO_3 and GG-PC/PAAm/ZnO_7) induced a slight improvement in thermal behavior compared with GG-PC/PAAm/ZnO_0 which may indicate strong interfacial interactions between ZnO and function groups of GG and PC the similar behavior was reported by Priyadarshi et al. with the addition of nZnO nanoparticles [33].

3.5 Factors Affecting the Swelling Capacity of GG-PC/PAAm/ZnO_x Composites

3.5.1 Effect of ZnO Concentration

Various concentrations of ZnO (wt%) are incorporated into GG-PC/PAAm/ZnOx hydrogel composite during preparation by gamma polymerization irradiation at a total exposure dose 10 kGy. The swelling performance of the prepared hydrogel composites versus zinc oxide concentration is represented in Fig. 4a. It can be depicted that there is a tremendous improvement in swelling performance as the percentage of incorporated zinc oxide increases. This improvement may be attributed to that the presence of ZnO nanoparticles causes penetration of more water molecules to balance the build-up ion osmotic pressure, which leads to swelling of the gel [34]. Furthermore, the presence of ZnO could expand the hydrogel network and increase the pores and free spaces within the networks, and as a consequence adsorbs more water [18].

3.5.2 Effects of Salinity

Figure 4b represents the swelling behaviors of GG-PC/PAAm/ZnO_0 and GG-PC/PAAm/ZnO_7 in solutions with different NaCl concentrations; 1.7, 3.4, 5.1, 6.8, 8.6 mmol/L. The swelling capacity of GG-PC/PAAm/ZnO_0 composite hydrogel is almost the same in distilled water and at lower salt concentration, up to 1 mmol/L. However, the swelling capacity was slightly increased within the range 1–3 mmol/L significantly decreased with increasing the concentration of the salt solutions. On the other hand, there is a dramatic decrease in the swelling percentage of GG-PC/PAAm/ZnO_7 when the salt concentration exceeds 3 mmol/L. This behavior can be explained on the basis of the charge screening effect in salt solution; the anion–anion electrostatic repulsion is responsible for a decrease in the osmotic pressure difference between gel network and the external solution [35]. Therefore, the osmotic pressure difference between the gel network and the external solution reduced with increase in the ionic strength of the saline concentration [36]. It can also be concluded that the hydrogel composite has high salt tolerance and can hold huge amount of water at relatively high salt concentration which fits the requirement of farming in salty and sandy soils.

3.5.3 Effect of pH

The swelling capacity of GG-PC/PAAm/ZnO_x hydrogel composite was studied at various pH solutions ranged from 1.0 to 11.0 as seen in Fig. 4c. The swelling capacities of both GG-PC/PAAm/ZnO_0 and GG-PC/PAAm/ZnO_7 hydrogel composites increase with increasing pH of the medium to get the maximum value at pH 9. Above this value a drop in the swelling capacity was observed. The carboxylic groups on the polymeric chains deprotonated with increasing the pH of the solution above the pKa value, which is 4.6. When the pH of the solution increased (5–9), some of –COOH groups are ionized and the electrostatic repulsion among negatively charged –COO– groups was increased which facilitates the relaxation of polymeric chains [37]. In addition, the hydrogen bonding interactions among the -COOH groups was partially broken because which widens the size of the network pores and thus

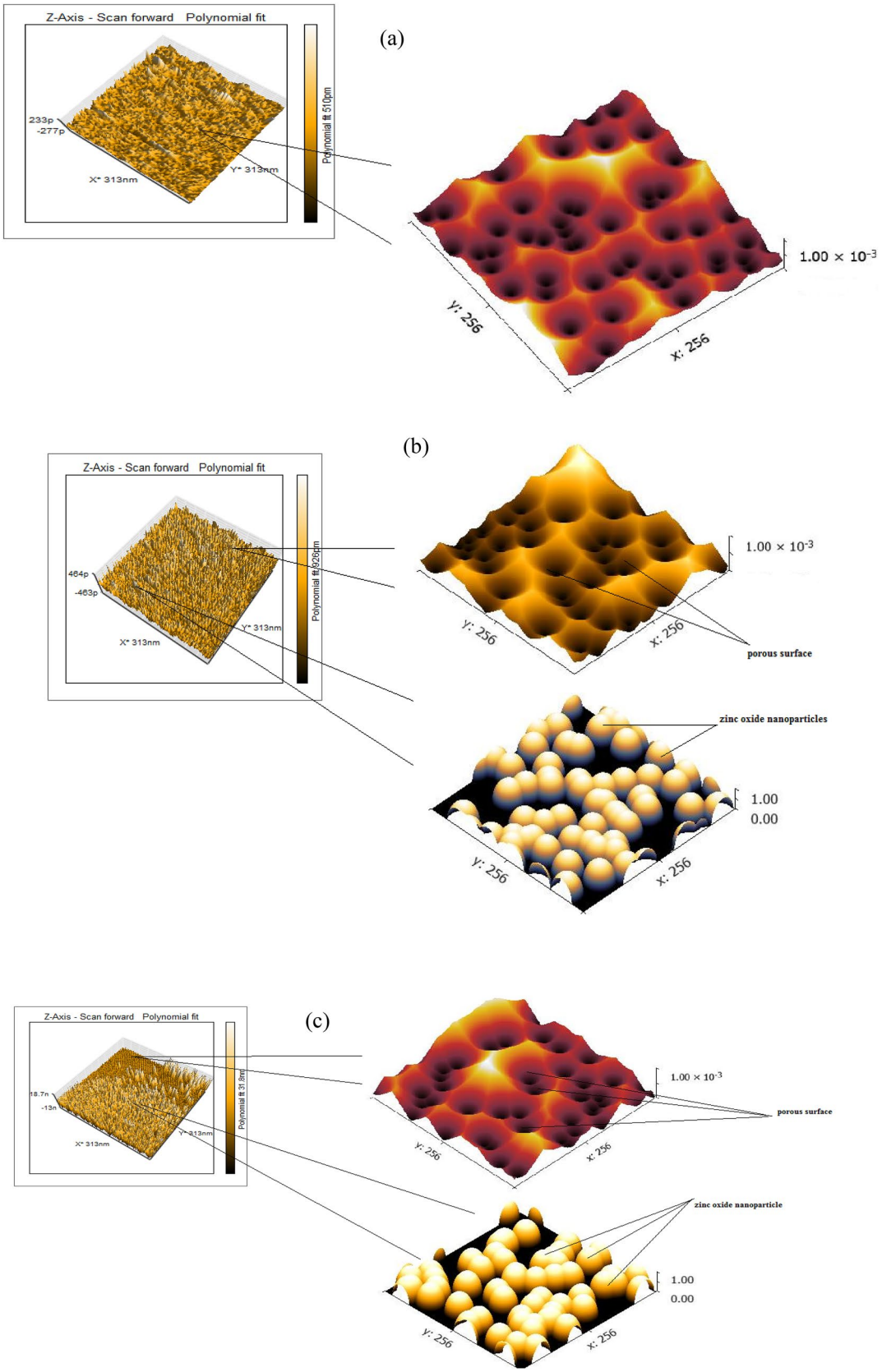

Fig. 2 AFM images of **a** GG-PC/PAAm/ZnO0, **b** GG-PC/PAAm/ZnO3, and **c** GG-PC/PAAm/ZnO7 hydrogel composites

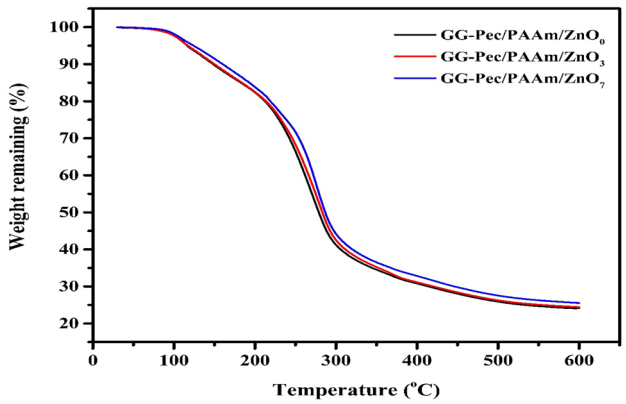

Fig. 3 TGA thermograms of GG-PC/PAAm/ZnO_0, GG-PC/PAAm/ZnO_3 and GG-PC/PAAm/ZnO_7

enhances the swelling capacity due to less crosslinked network structure. However, at much higher pH (> 10), the 'charge screening effect' of excess Na + in the swelling medium restricts the net charges of –COO– anions and prevents effective anion–anion repulsion so swelling decreased [37].

3.5.4 Effect of Temperature

The swelling behavior of GG-PC/PAAm/ZnO_0 and GG-PC/PAAm/ZnO_7 was verified at temperature range 30, 45, and 55 °C, Fig. 4d. It was found that increasing temperature resulted in increasing the swelling capacity of the investigated hydrogel composites. This may be explained by that the increase in temperature causes an increase in the diffusion and penetration of water into the pores existing within the hydrogel matrix.

3.6 Swelling Kinetics

The swelling capacity of GG-PC/PAAm/ZnO_0 and GG-PC/PAAm/ZnO_7 was investigated as a function of time as shown in Fig. 5a. It is observed that the swelling capacity of all hydrogels increases progressively within the time of swelling up to 500 min, thereafter it levels off. The swelling kinetic parameters GG-PC/PAAm/ZnO_0 hydrogel, and PC-GG/PAAm/ZnO_7 hydrogel composite were investigated. The mechanism of the water transportation through the prepared hydrogel and nanocomposite was obtained by applying the following relationships [38, 39].

$$F = \frac{M_t}{M_{eq}} = kt^n \tag{6}$$

$$\ln F = \ln k + n \ln t \tag{7}$$

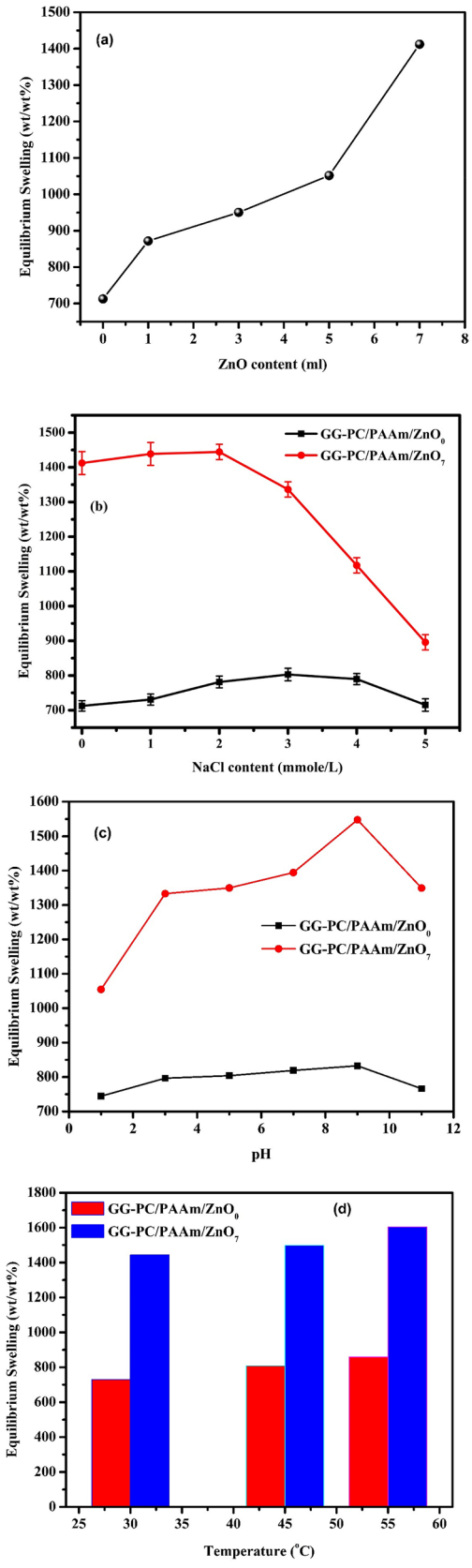

Fig. 4 Equilibrium Swelling (wt/wt%) of GG-PC/PAAm/ZnO_x at different: **a** ZnO content, **b** NaCl content; **c** pH values and **d** temperatures (°C)

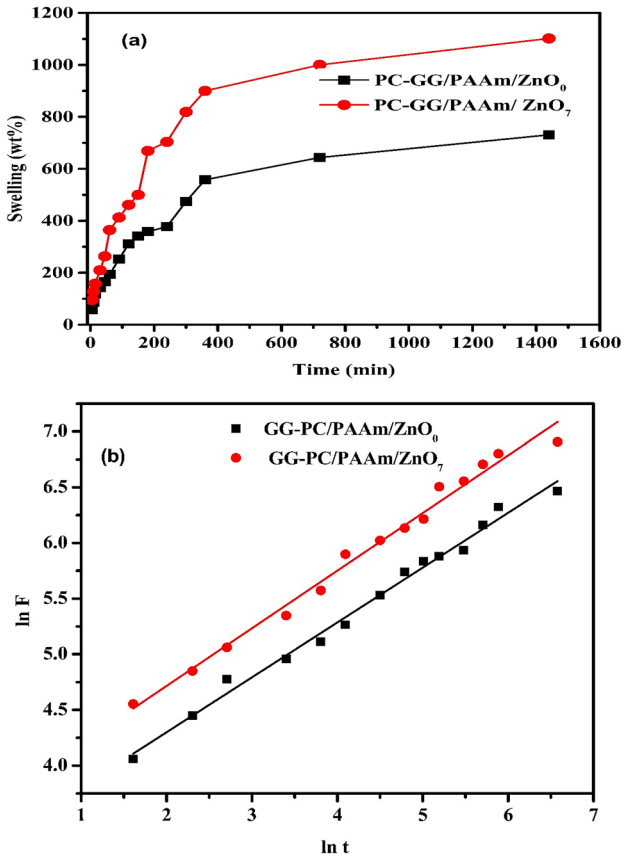

Fig. 5 **a** Swelling percentage of GG-PC/PAAm/ZnO_0 and GG-PC/PAAm/ZnO_7 hydrogel composite at different time intervals in distilled water. **b** Swelling kinetic curves for GG-PC/PAAm/ZnO_0 hydrogel, and PC-GG/PAAm/ZnO_7 hydrogel composites

k is the diffusion constant (dependent on hydrogel type and swelling medium) incorporating characteristic of the polymeric network system., n is the diffusion exponent (which provides information regarding the transport mechanisms that drive the sorption of a particular solute), and M_t and M_{eq} are hydrogel masses at a swelling time t and at equilibrium, respectively.

The Fick law (Eq. 6) was applied on GG-PC/PAAm/ZnO_0 and PC-GG/PAAm/ZnO_7 composite hydrogels as shown in Fig. 5b and the obtained data are summarized in Table 2. The nature of the water diffusion process depends on the value of n. When n less than 0.5, the swelling mechanism is controlled by diffusion, when the value of n is between $0.5 < n < 1$, the system is controlled by diffusion and relaxation. According to the values of n, GG-PC/PAAm/ZnO_0 hydrogel is Fickian diffusion while PC-GG/PAAm/ZnO_7 hydrogel composite is non-Fickian diffusion. This means that ZnO controls in the mechanism of swelling.

Table 2 Values of swelling coefficients of GG-PC/PAAm/ZnO_0 and PC-GG/PAAm/ZnO_7 hydrogel composite

Sample	n	K (min^{-1})	R^2
PC-GG/PAAm/ZnO_0	0.49 ± 0.014	27.51 ± 1.76	0.9904
PC-GG/PAAm/ZnO_7	0.52 ± 0.017	39.62 ± 3.16	0.9873

3.7 Amendment of Physical Properties of the Soil with GG-PC/PAAm/ZnO_7 Composite

3.7.1 Water Holding Capacity (WHC)

The WHC% of soil with various amounts of the PC-GG/PAAm/ZnO_7 hydrogel composite (1, 2, and 3%) are represented in Fig. 6a. The WHC% of soil without composite (0%) is 15%, whereas the WHC% of the treated soil is 25%, 49% and 61%for PC-GG/PAAm/ZnO_7 of 1%, 2% and 3%, respectively. The soil can catch and keep a significant amount of water as the amount of added composite material is increased. As a result, soil moisture is amended, and water consumption is diminished. This finding confirms the outstanding efficiency of the claimed hydrogel composite in modifying the physical nature of the sand soil used in this study. This result can be discussed on the basis of the hydrophilic nature of PC-GG/PAAm/ZnO_7 [34]. Moreover, the highly porous structure and high surface area of PC-GG/PAAm/ZnO_7 as proved by the AFM images enhance water holding of the soil by capturing a huge amount of water within its voids. The water holding capacity of the prepared hydrogels was compared over similar materials in terms of maximum amount of absorbed water, the data are given in Table 3.

3.7.2 Water Retention (WR)

Figure 6b depicts the effect of different concentrations of the superabsorbent hydrogel composites PC-GG/PAAm/ZnO_0 and PC-GG/PAAm/ZnO_7 on the water retention of the sandy soil. It can be seen that WR of blank soil decreases, with all the irrigated water lost over 7 days, while the WR% of the soil mixed with any concentration of the prepared composite was down after 18 and 20 days for 3% of PC-GG/PAAm/ZnO_0 and PC-GG/PAAm/ZnO_7, respectively. Therefore, the water retention rate of the soil was improved by adding 3% of the composite. It is also clear that soil amendment achieved by PC-GG/PAAm/ZnO_7 is more pronounced than that of PC-GG/PAAm/ZnO_0. This behavior may be attributed to that the PC-GG/PAAm/ZnO_x hydrogel composites possessing a high hydrophilic structure with numerous hydrophilic

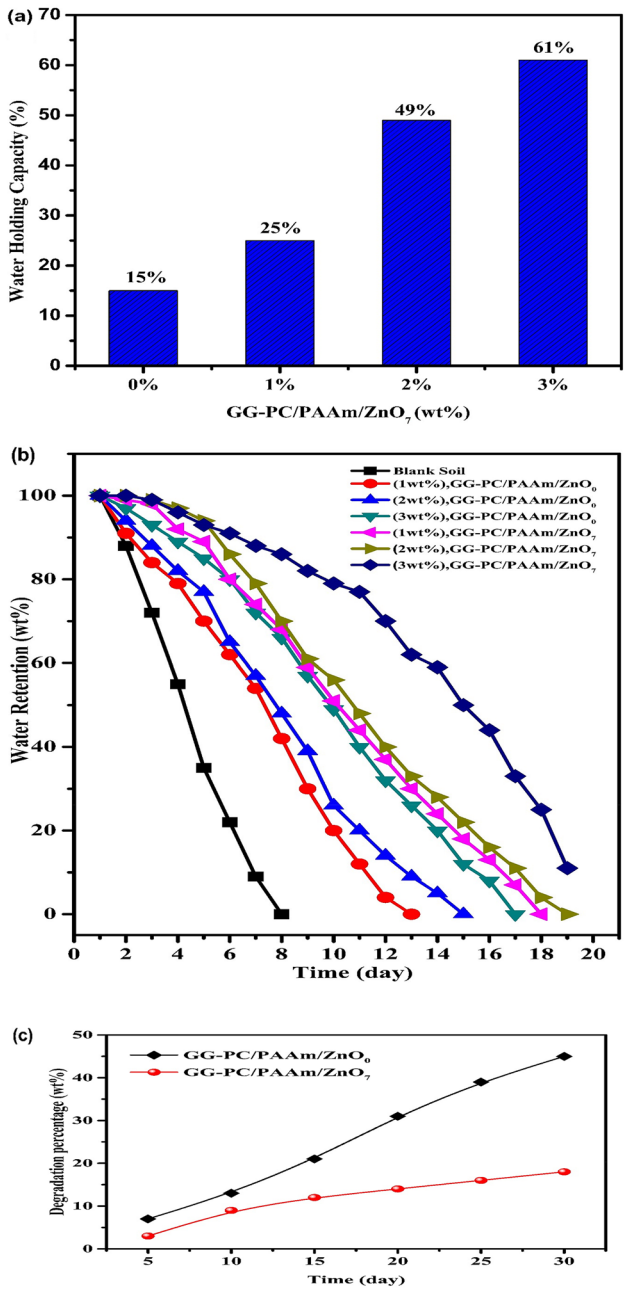

Fig. 6 **a** Effect of GG-PC/PAAm/ZnO_7 composite hydrogel content (wt%) on water holding capacity of the investigated soil (wt%). **b** Effect of different content of the superabsorbent composite hydrogels GG-PC/PAAm/ZnO_0 and GG-PC/PAAm/ZnO_7 on the water retention of the sandy soil. **c** Degradation percentage (%) of GG-PC/PAAm/ZnO_0 and GG-PC/PAAm /ZnO_7 hydrogel composite

groups that can capture water molecules by hydrogen bonding formation. In addition, the effective porosity and high surface area aid in absorbing and retaining a huge amount of water.

3.8 Biodegradation in Sandy Soil

The rate of biodegradation of GG- PC/PAAm/ZnO_0 and GG-PC/PAAm/ZnO_7 is illustrated in Fig. 6c. It is clear that the GG-PC/PAAm/ZnO_0 exhibited fast degradation, i.e., about 45% of the mass of the incubated hydrogel was degraded after 30 days of the experiment due ot its high content of the green polymers. On the other hand, GG-PC/PAAm/ZnO_7 showed high resistance to the biodegradation due to the antimicrobial activity of ZnO [44].

3.9 Reusability Study

The maximum water absorption of GG-PC/PAAm/ZnO_0 and GG-PC/PAAm/ZnO_7 was estimated at three swelling/deswelling cycles in order to investigate the reusability of these hydrogels. The data are presented in Fig. 7. It is clear that the composite hydrogel GG-PC/PAAm/ZnO_7 can be repeatedly used with reasonable swelling capacity when compared with PC/PAAm/ZnO_0. This observation may be due to the role of ZnO in reserving the hydrogel structure and protecting the gel matrix during repeated swelling/deswelling cycles [45]. Repeated use of hydrogel with acceptable performance is very important for economic efficiency and sustainable agriculture.

4 Conclusions

Green superabsorbent hydrogel composites were prepared and employed for sustained agriculture. The hydrogels comprised of guar gum, pectin and acrylamide crosslinked together with gamma irradiation and fabricated with different weight ratios of zinc oxide. The chemical structure of the composites was proved by the FT-IR and their topography was scanned by the AFM. The data reveal that the composite GG-PC/PAAm/ZnO_7 depicted maximum swelling, high water retention and the lowest degradation due to the presence of zinc oxide which possess well-established antibacterial effect. Moreover, the swelling kinetics reveal that GG-PC/PAAm/ZnO_0 hydrogel follows Fickian diffusion while PC-GG/PAAm/ZnO_7 hydrogel composite obeys non-Fickian diffusion. This proves that ZnO controls in the mechanism of swelling. The results also confirmed the high efficiency of the prepared composites in amending the physical properties of sandy soil. So that they can be employed as excellent candidates in sustained agriculture.

Table 3 Water holding capacity of different hydrogels

Hydrogel material	Water holding capacity	References
Guar gum-g-poly(sodium acrylate) (GG-g-PNaA) superabsorbent hydrogels	1107 g g^{-1} in distilled water and 88 g g^{-1} in 0.9 wt% NaCl solution	[40]
Guar gum grafted with acrylic acid and cross-linking with ethylene glycol di meth-acrylic acid (EGDMA)	800 g g^{-1} in distilled water	[41]
Cross linked guar gum-g-poly(acrylate)	325 g g^{-1} in distilled water	[42]
Pectin/glycidyl methacrylate hydrogel	643.67 g g^{-1} in distilled water	[43]
Guar gum/Pectin/Zinc oxide)	1450 g g^{-1} in distilled water, 800 g g^{-1} in 3 mmol/L NaCl	The present work

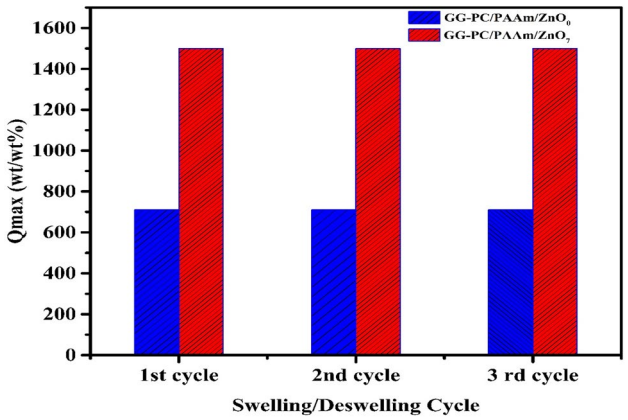

Fig. 7 Maximum water absorption capacity (Qmax,wt/wt%) of GG-PC/PAAm/ZnO_0 and GG-PC/PAAm/ZnO_7 hydrogel composite at three swelling/deswelling cycles

Author Contributions AS: Conceptualization, Methodology, Investigation, Data presentation, Validation. MM: Conceptualization, Methodology, MA-R: Writing & editing, Supervision, Validation, AFM: Investigation. GA: Investigation, Validation. Writing—review & editing, Supervision.

Funding Open access funding provided by The Science, Technology & Innovation Funding Authority (STDF) in cooperation with The Egyptian Knowledge Bank (EKB). The authors declare that no funds, grants, or other support were received during the preparation of this manuscript.

Data Availability The datasets generated during and/or analysed during the current study are available from the corresponding author on reasonable request.

Declarations

Conflict of interest The authors declare that they have no known competing financial interests or personal relationships that could have appeared to influence the work presented in this manscript.

References

1. O. Schmidt, S. Padel, L. Levidow, The bio-economy concept and knowledge base in a public goods and farmer perspective. Bio-based Appl. Econ. **1**(1), 47–63 (2012)
2. B. Han, S.G. Benner, A.N. Flores, Evaluating impacts of climate change on future water scarcity in an intensively managed semi-arid region using a coupled model of biophysical processes and water rights. Hydrol. Earth Syst. Sci. Discuss. **9**, 1–53 (2018)
3. !!! INVALID CITATION !!! [3–8].
4. R.L. Shrestha et al., Washnut seed-derived ultrahigh surface area nanoporous carbons as high rate performance electrode material for supercapacitors. Bull. Chem. Soc. Jpn. **94**(2), 565–572 (2021)
5. X. Sheng et al., Nitrogenization of biomass-derived porous carbon microtubes promotes capacitive deionization performance. Bull. Chem. Soc. Jpn. **94**(5), 1645–1650 (2021)
6. Z. Lou et al., Biomass-derived carbon heterostructures enable environmentally adaptive wideband electromagnetic wave absorbers. Nano-micro Lett. **14**(1), 1–16 (2022)
7. H. Karimi-Maleh et al., Nanochemistry approach for the fabrication of Fe and N co-decorated biomass-derived activated carbon frameworks: a promising oxygen reduction reaction electrocatalyst in neutral media. J Nanostruct. Chem. (2022). https://doi.org/10.1007/s40097-022-00492-3
8. B. Das, S. Paul, H.K. Sharma, A review on bio-polymers derived from animal sources with special reference to their potential applications. J. Drug Deliv. Ther. **11**(2), 209–223 (2021)
9. M.E. Abdel-Raouf et al., Green chemistry approach for preparation of hydrogels for agriculture applications through modification of natural polymers and investigating their swelling properties. Egypt. J. Pet. **27**(4), 1345–1355 (2018)
10. A. Abdelaziz et al., Preparation and characterization of a new family of bio-interpenetrating network hydrogel based on a green method. Egypt. J. Chem. **64**(12), 7451–7464 (2021)
11. M.A. Qureshi et al., Polysaccharide based superabsorbent hydrogels and their methods of synthesis: a review. Carbohydr. Polym. Technol. Appl. **1**, 100014 (2020)

12. M.R. Guilherme et al., Superabsorbent hydrogels based on polysaccharides for application in agriculture as soil conditioner and nutrient carrier: a review. Eur. Polym J. **72**, 365–385 (2015)
13. R. Vundavalli et al., Biodegradable nano-hydrogels in agricultural farming-alternative source for water resources. Procedia Mater. Sci. **10**, 548–554 (2015)
14. M. Premsekhar, V. Rajashree, Influence of bio-fertilizers on the growth characters, yield attributes, yield and quality of tomato. Am.-Eurasian J. Sustain. Agric. **3**(1), 68–70 (2009)
15. M. Nasrollahzadeh et al., Starch, cellulose, pectin, gum, alginate, chitin and chitosan derived (nano) materials for sustainable water treatment: a review. Carbohydr. Polym. **251**, 116986 (2021)
16. !!! INVALID CITATION !!! [15–18].
17. A. Anjum et al., Preparation and characterization of guar gum based polyurethanes. Int. J. Biol. Macromol. **183**, 2174–2183 (2021)
18. H. Namazi, M. Hasani, M. Yadollahi, Antibacterial oxidized starch/ZnO nanocomposite hydrogel: synthesis and evaluation of its swelling behaviours in various pHs and salt solutions. Int. J. Biol. Macromol. **126**, 578–584 (2019)
19. R. Beli et al., Chemistry and uses of pectin—a review critical reviews. Food Sci. Nutr. **37**(1), 47–73 (1997)
20. P. Sriamornsak, Chemistry of pectin and its pharmaceutical uses: a review. Silpakorn Univ. Int. J. **3**(1–2), 206–228 (2003)
21. G.A. Mahmoud et al., Chitosan biopolymer based nanocomposite hydrogels for removal of methylene blue dye. SN Appl. Sci. **2**(5), 1–10 (2020)
22. A. Sayed et al., Characterization and optimization of magnetic Gum-PVP/SiO2 nanocomposite hydrogel for removal of contaminated dyes. Mater. Chem. Phys. **280**, 125731 (2022)
23. I. Călina et al., One step e-beam radiation cross-linking of quaternary hydrogels dressings based on chitosan-poly (vinylpyrrolidone)-poly (ethylene glycol)-poly (acrylic acid). Int. J. Mol. Sci. **21**(23), 9236 (2020)
24. M.Y. Sayah et al., Yield, esterification degree and molecular weight evaluation of pectins isolated from orange and grapefruit peels under different conditions. PLoS ONE **11**(9), e0161751 (2016)
25. V. Hasija et al., Green synthesis of agar/gum Arabic based superabsorbent as an alternative for irrigation in agriculture. Vacuum **157**, 458–464 (2018)
26. R. Sahraei, M. Ghaemy, Synthesis of modified gum tragacanth/graphene oxide composite hydrogel for heavy metal ions removal and preparation of silver nanocomposite for antibacterial activity. Carbohydr. Polym. **157**, 823–833 (2017)
27. N. Nagasawa et al., Radiation crosslinking of carboxymethyl starch. Carbohydr. Polym. **58**(2), 109–113 (2004)
28. L.S. Tan et al., Fabrication of radiation cross-linked diclofenac sodium loaded carboxymethyl sago pulp/chitosan hydrogel for enteric and sustained drug delivery. Carbohydr. Polym. Technol. Appl. **2**, 100084 (2021)
29. D. Mudgil, S. Barak, B. Khatkar, X-ray diffraction, IR spectroscopy and thermal characterization of partially hydrolyzed guar gum. Int. J. Biol. Macromol. **50**(4), 1035–1039 (2012)
30. A.S. Al-Gorair, A. Sayed, G.A. Mahmoud, Engineered superabsorbent nanocomposite reinforced with cellulose nanocrystals for remediation of basic dyes: isotherm, kinetic, and thermodynamic studies. Polymers **14**(3), 567 (2022)
31. A.S. Jain et al., Bionanofactories for green synthesis of silver nanoparticles: toward antimicrobial applications. Int. J. Mol. Sci. **22**(21), 11993 (2021)
32. M.E. Keshawy, R.S. Kamal, M. Abdel-Raouf, Synthesis and investigation of green hydrogels for simultaneous removal of mercuric cations and methylene blue from aqueous solutions. Egypt. J. Chem. **65**(5), 1–2 (2022)
33. R. Priyadarshi, S.-M. Kim, J.-W. Rhim, Carboxymethyl cellulose-based multifunctional film combined with zinc oxide nanoparticles and grape seed extract for the preservation of high-fat meat products. Sustain. Mater. Technol. **29**, e00325 (2021)
34. M. Yadollahi et al., Synthesis and characterization of antibacterial carboxymethyl cellulose/ZnO nanocomposite hydrogels. Int. J. Biol. Macromol. **74**, 136–141 (2015)
35. X. Shi, W. Wang, A. Wang, Synthesis and enhanced swelling properties of a guar gum-based superabsorbent composite by the simultaneous introduction of styrene and attapulgite. J. Polym. Res. **18**(6), 1705–1713 (2011)
36. Y.M. Mohan, P.K. Murthy, K.M. Raju, Synthesis, characterization and effect of reaction parameters on swelling properties of acrylamide–sodium methacrylate superabsorbent copolymers. React. Funct. Polym. **63**(1), 11–26 (2005)
37. G.A. Mahmoud et al., Characterization and properties of magnetic and non-magnetic (Gum Acacia/Polyacryamide/Graphene) nanocomposites prepared by gamma irradiation. J. Inorg. Organomet. Polym Mater. **28**(6), 2633–2644 (2018)
38. E.E. Khozemy, S.M. Nasef, G.A. Mahmoud, Synthesis and characterization of antimicrobial nanocomposite hydrogel based on wheat flour and poly (vinyl alcohol) using γ-irradiation. Adv. Polym. Technol. **37**(8), 3252–3261 (2018)
39. Sayed, A., et al., Green starch/graphene oxide hydrogel nanocomposites for sustained release applications. Chem. Pap. **76**, 5119–5132 (2022)
40. Wang, W.B. and A.Q. Wang. *Preparation, swelling and water-retention properties of crosslinked superabsorbent hydrogels based on guar gum*. In: *Advanced Materials Research*. 2010. Trans Tech Publ.
41. N. Thombare et al., Design and development of guar gum based novel, superabsorbent and moisture retaining hydrogels for agricultural applications. Carbohydr. Polym. **185**, 169–178 (2018)
42. K.P. Chandrika et al., Novel cross linked guar gum-g-poly (acrylate) porous superabsorbent hydrogels: characterization and swelling behaviour in different environments. Carbohydr. Polym. **149**, 175–185 (2016)
43. M.R. Guilherme et al., Pectin-based polymer hydrogel as a carrier for release of agricultural nutrients and removal of heavy metals from wastewater. J. Appl. Polym. Sci. **117**(6), 3146–3154 (2010)
44. S.-E. Jin, H.-E. Jin, Antimicrobial activity of zinc oxide nano/microparticles and their combinations against pathogenic microorganisms for biomedical applications: from physicochemical characteristics to pharmacological aspects. Nanomaterials **11**(2), 263 (2021)
45. A.H.A. Saad et al., Removal of toxic metal ions from wastewater using ZnO@ chitosan core-shell nanocomposite. Environ. Nanotechnol. Monit. Manag. **9**, 67–75 (2018)